Progress in Chemical and Biochemical Research

Original Research Article

Ag-nanoparticles Mediated by *Lonchocarpus laxiflorus Stem Bark* Extract as Anticorrosion Additive for Mild Steel in 1.0 M HCl Solution

Godwin Abawulo Ijuo*, Surma Nguamo, John Ogbaji Igoli

Department of Chemistry, Federal University of Agriculture, PMB, 2373, Makurdi, Benue State, Nigeria

A R T I C L E   I N F O

A B S T R A C T

Green synthesis of silver nanoparticles using stem bark extract of *Lonchocarpus laxiflorus* plant as a reducing agent following a simple, effective, and eco-friendly route was reported in this work. UV-vis, FTIR SEM/EDX, and Backscatter Electron Detector (BSD) analysis were employed in the characterisation of the nanoparticles synthesised. The dispersed nanoparticles were found to have mean particle size of 2.3 nm. The resultant nanoparticles were tested for corrosion inhibition potential of mild steel as a possible alternative to the expensive and environmentally harmful inorganic inhibitors. The composite has proven to be effective inhibitor of corrosion of mild steel in 1.0 M HCl. Further treatment of the experimentally determined results showed that the values of the activation energies were all less than 80 KJmol^{-1}, indicating physical adsorption of the composite to the mild steel surface according to Langmuir's isotherm. The behaviour of this mixed-type inhibitor was endothermic in nature and followed associative mechanism.
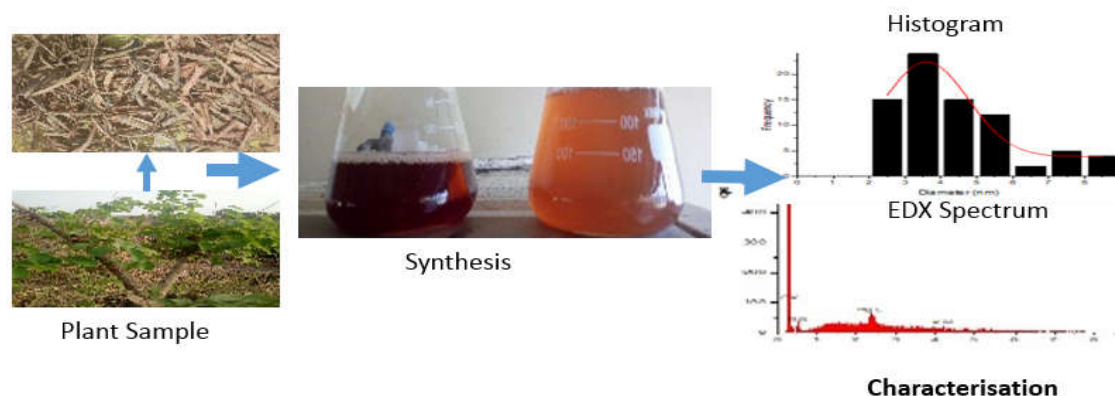
* Corresponding author: Godwin Abawulo Ijuo

✉ E-mail: ijuogodwin@gmail.com

☎ Tel number: +2348131837423

G R A P H I C A L A B S T R A C T

1. Introduction

Metals in service are chemically unstable in an aggressive environment including air, air-saturated water, and sometimes air-free water at ambient temperatures, except gold. This implies the potential hostility of almost all environments in which metals are used. It is therefore largely dependent on the protective mechanisms for the successful application of metals in engineering and commercial purpose, which when overlooked, the metal becomes vulnerable to attack, resulting in break down, exhaustion, and corrosion [1-2].

Mild steel is one of the best preferred construction material for industries and many other areas, especially where strength, weight, thermal, and electrical requirements are primary technological considerations. Because of its mechanical properties, excellent thermal and electrical conductivity, availability, malleability, and ductility among others, it is highly endeared to users. However, it is highly prone to corrosion, especially when it comes in contact with aggressive solutions such as acids which are commonly used in several oilfield operations in pipelines; storage tanks, etc. [2-3]. This action generally makes metallic components susceptible to corrosion during industrial processes. The appropriate corrosion control mechanism should be adopted to minimize corrosion of the industrial equipment and facilities. Without

proactive solution to corrosion, metal damage or deterioration often occurs after it has been implemented into service. Correcting unanticipated corrosion during the operational phase of the lifecycle is both probable and can be very costly, except replacing troubled components or structures at great expense [4] Report has it that average of $765 million is lose annually to corrosion of oil pipelines by the oil and gas industry in Nigeria alone, with chemical treatment as the most expensive cost contribution of 81 % of the entire cost, while coating gulps the balanced 19 % cost of prevention. For the contribution of corrosion maintenance methods, 60 % goes for repairs while 40 % for replacement [5]. Worst still is the fact that some chemical substances used in this control of corrosion are not eco-friendly and poses adverse effect to man and his environment. Plant extracts as corrosion inhibitor remains the cheapest, the eco-friendliest, more readily available, and renewable alternative to the several methods of corrosion control and prevention such as material selection, coating, cathodic protection, etc. [6-7].

Nanotechnology has many exciting applications with its unique advances and may be easily merged with the other technologies with some modifications. The use of nanostructured materials has provided an increased surface area for higher reaction rate which has been exploited

in various fields like agriculture, environment, biotechnology, medicine, drug delivery textile, food, and energy [8].

Nano-materials are known to have the ability to form self-assembled films on the metal surfaces, and have thus attracted tremendous interest not only as corrosion inhibitor, but also in science, in general. Silver nanoparticles have found wide application as corrosion inhibitor due to their high reactivity towards aqueous acidic solution [9]. In recent times, composites formed between nanoparticles and organic molecules have been reported to be effective in inhibiting corrosion of mild steel in acidic environments [10-13].

Lonchocarpus laxiflorus is a species of legume in the Fabaceae family. It is called folahi in Hausa and uhia in Igede. The tree grows to 4–8 meters in height, has grey or yellowish bark and compound leaves. The new leaves are accompanied by purple flowers on multi-branched pinnacles. The fruit is glabrous paper pod, usually containing one seed. *Lochocarpus laxiflorus* is widely distributed in West Africa, Central Africa, the African Great lakes, and North Africa. It is found in savannah woodlands and dry forested areas, particularly fringing forest near water sources. It is used across its range for traditional medicine [14]. There are very few literatures on plant extracts-nanoparticles composite used as corrosion inhibitor. In recent times, composites formed between nanoparticles and organic molecules (polymers) have been reported to be effective in inhibiting corrosion of mild steel in acidic environments. However, to the best of my knowledge there is no report on *lonchocarpus laxiflorus* extracts-nanoparticles composite used as corrosion. This has therefore necessitated thoughts for research along these lines.

2. Materials and Methods

2.1. Collection of plants

The stem barks of *Lonchocarpus laxiflorus* (LL) specimen were collected in Benue State, and were identified at Botany Department, Federal University of Agriculture Makurdi, Nigeria.

2.2. Preparation of Plant Extracts

The fresh stem barks were air dried for six weeks, then blended into fine powder and the samples stored in a polyethylene bag for extraction. N-hexane was first used to extract 100 g of the fine powdered samples at room temperature by macerating for 72 h. After filtration with whatman filter paper No. 1 using a vacuum pump, the residue was subsequently re-extracted with ethyl acetate and with methanol, respectively and they were macerated for 72 hours in each of the solvents. All the solvents used, though analytical grade, were redistilled once before use. The solvents were completely removed using rotary evaporator, leaving dry extracts, which were stored in dark bottles at 5 °C until usage.

2.3. *Lonchocarpus laxiflorus* extract-silver nanoparticles (LLE-AgNPs) Synthesis

The procedure for the synthesis of LLE-AgNPs was similar to those reported by Shameli *et al.* (2012) [15]. This synthesis was carried out based on the principle that silver nitrate solution can be reduced using plant extracts as a reducing agent. To this end, 100 mL de-ionized water was added to 1 g of the plant extract and the mixture was stirred vigorous for 1 h. This was followed by adding 100 mL of 1 mM $AgNO_3$ and mixed at 25 °C for 48 h. Colour change was observed for the period of the synthesis. After centrifuging to separate the products using centrifuge, the supernatant was discarded and the pellets were collected and stored.

2.4. Gravimetric measurement

The 2 x 3 cm dimension mild steel coupon were brushed with silicon carbide abrasive paper, followed by degreasing with acetone, then rinsed with distilled water and weighed. This was immediately followed by the immersion of the pre-weighed mild steel coupons in 200 mL of 1.0 M HCl. Tests were carried out at 303, 313, 323,

and 333 K, respectively for 3 hours of immersion using 100 ppm, 300 ppm, and 500 ppm LLE-AgNPs in order to investigate the effect of temperature. The difference between the initial weights and the final weight of the coupon at a given time was taken to be the weight loss. All tests were run in duplicate. The inhibition efficiency (%IE) and corrosion rate of mild steel were calculated from the weight loss results, according to equation 1 [16].

$$IE_{exp} = \left(1 - \frac{W_{(1)}}{W_{(0)}}\right)x100 \qquad (1)$$

In which, $W_{(0)}$ is the weight loss of the mild steel without inhibitor and $W_{(1)}$ is the weight loss of mild steel with inhibitor.

$$CR\left(gh^{-1}cm^{-2}\right) = \frac{\Delta W}{At} \qquad (2)$$

2.5. Potentiodynamic Polarization Study (PDP)

The mild steel was used as working electrode was automatically polarized from -300 mV to 300 mV with a scanning rate of 1 mV/s. The points to corrosion potential Ecorr were extrapolated to obtain corrosion current density (icorr). The inhibition efficiency (%IE) was obtained from Equation 3.

$$\%IE = \frac{I_{corr(i)} - I_{corr(f)}}{I_{corr(i)}} \times 100 \qquad (3)$$

In which, $I_{corr(f)}$ and $I_{corr(i)}$ are the corrosion current densities of MS with and without the inhibitor, respectively.

2.6. Surface morphologies and elemental composition

The surface morphologies and elemental compositions of LLE-AgNPs were investigated using a UV-visible spectrophotometer, Scanning Electron Microscopy (SEM)/Energy Dispersive X-ray Analysis (EDX), Backscatter electron Detector (BSD) analysis, and Transformed Infrared (FTIR) Spectroscopy. The FTIR of the LLE-AgNPs and that of the corrosion was carried out using FTIR-8400S at 303 K.

3. Results and Discussion

3.1. Synthesis and characterization

The Ag+ reduction was confirmed by the apparent change in color of the reaction mixture from pale to yellowish brown (**Figure 1**). The excitation of Surface Plasmon vibration in silver nanoparticles has been reported to be responsible for such change in color [17].
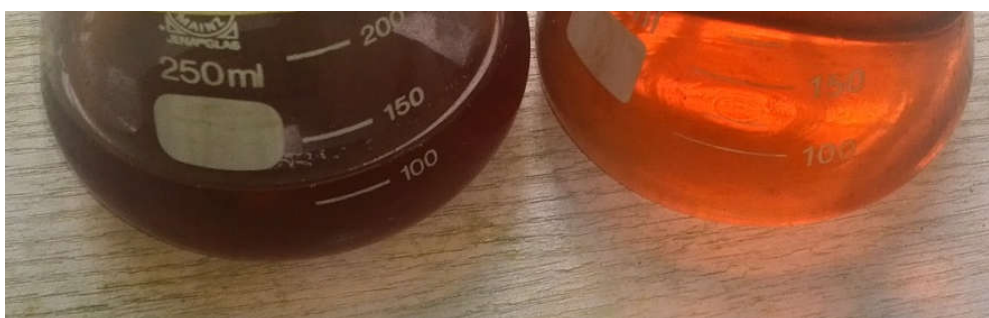

Figure 1. Observed colour change after 48 hours

UV analysis showed a peak at 416 nm (**Figure 2**) that suggested the presence of AgNPs due to surface plasmon resonance [18]. The previous studies suggest that smaller particles of sizes ranging from 5-10 nm absorb UV/Vis light near 420 nm [19]. Less single surface plasmon resonance possessed by smaller nanoparticles

are said to result in blue shift [20-21]. This suggests from λ_{max} at 416 nm that the synthesized LLE-AgNPs have small sizes, less than 20 nm. SEM images (**Figure 3**) also supported this argument. LLE-AgNPs were mostly poly-dispersed quasi-spherical in shape

with very slight size differences, evenly distributed in the plant extract.
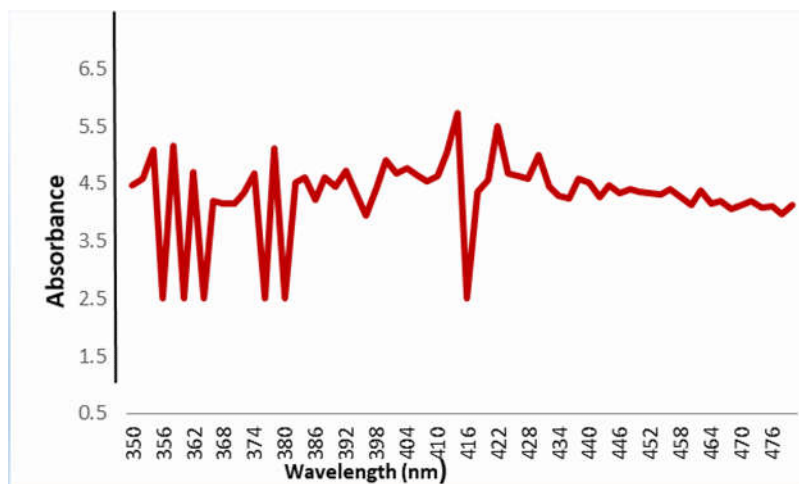

**Figure 2.** UV-Vis absorption spectrum images for LLE-AgNPs

The mean size (Xc) was revealed to be 2.3 nm, width (w) to be 0.9, Area (A) to be 34.9, and the offset (y0) to be 3.2 as shown in the histogram plot of the SEM analysis in **Figure 3**, with dispersity of 5.68%, implying none uniformity of the nanoparticles sizes. The nanoparticles are therefore colloidal crystals. According to Law and Kelton 1991 [22], simulation shows that such dispersed nanoparticles will require higher compressions to freeze the suspension and that crystallization is suppressed in suspension. This is attributable to thermodynamic factors. Further mapping of the inter-dispersion of LL-AgNPs using Backscatter electron detector (BSD) analysis (**Figure 6),** shows no clear particle aggregation in the cross sections of the composites, indicating that the LL-AgNPs were well dispersed, a result similar to that reported by Benhabiles *et al.* [23].

The EDX analysis shows visible peaks as shown in **Figure 4,** confirming the presence of carbon, nitrogen, oxygen, silver and magnesium elements in the sample.
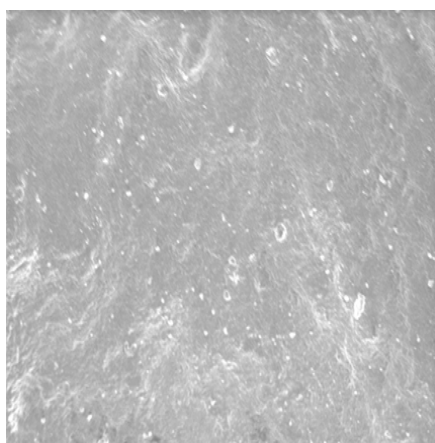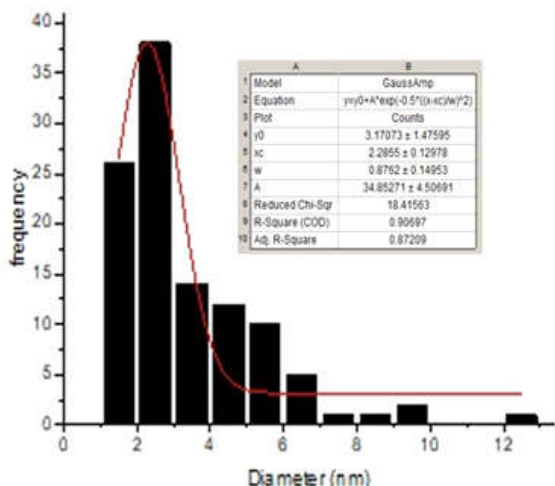

Figure 3. SEM Images showing the surface morphology for LL-AgNPs
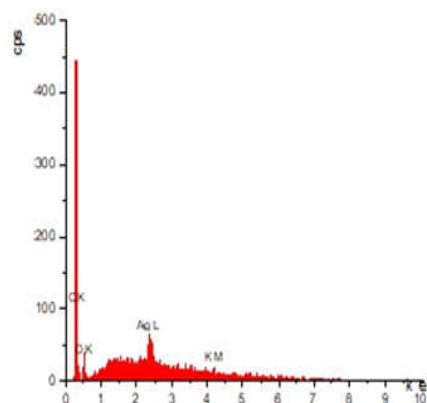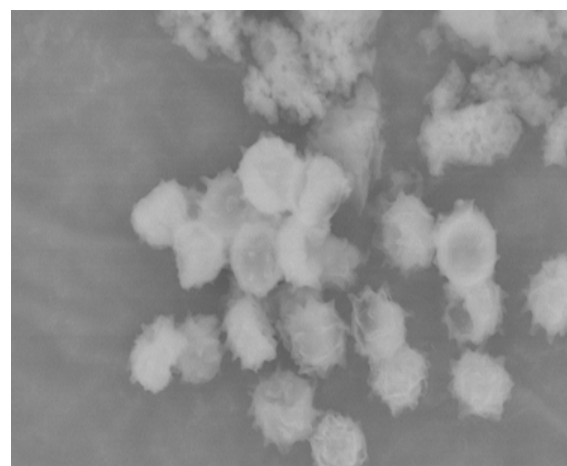

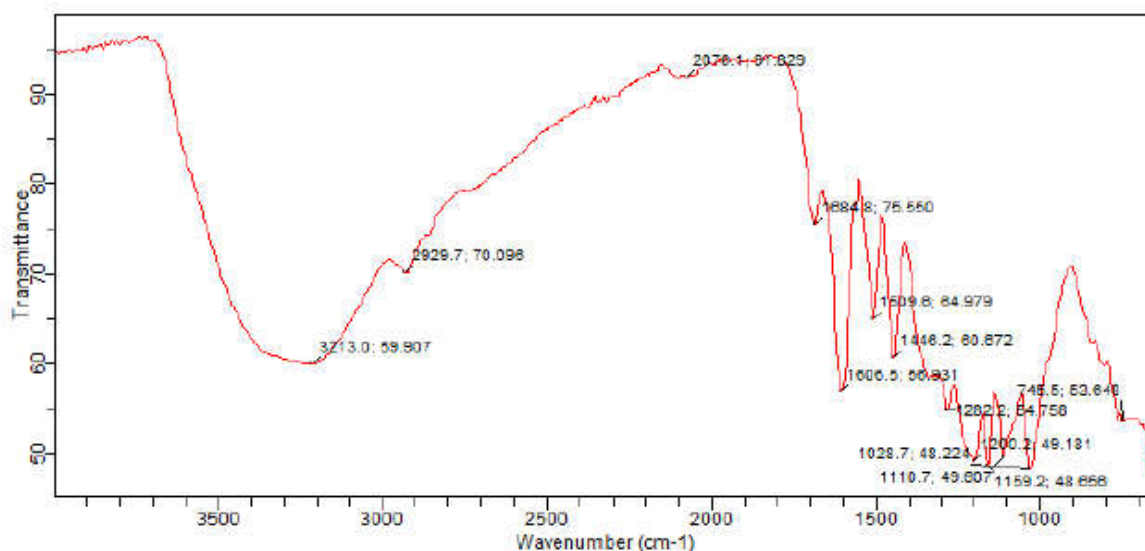**Figure 4.** EDX characteristic spectrum obtained for LLE-AgNPs

Figure 5. Histogram plot from the EDX spectrum for LLE-AgNPs

Figure 6. SEM-BSD (backscatter electron detector) pictures for LL-AgNPs distribution

Figure 7. FTIR spectrum of from LLE-AgNPs

The band at 3213 corresponds to N-H amide, 2929 is due to O-H of carboxylic acid. The bands between 1684-1446 are attributed to C=C aromatic stretching vibration. 1282-1200 corresponds to C-O ester Sp2, while the bands at 1159, 1110, 1028, and 745 are due to C-N amine, C-O alcohol, C-O esters Sp3, and C-Cl alkylhalides vibrations, respectively. It can be inferred that the reducing and stabilizing agents are the hydroxyl and carbonyl groups presented in the sample [24].
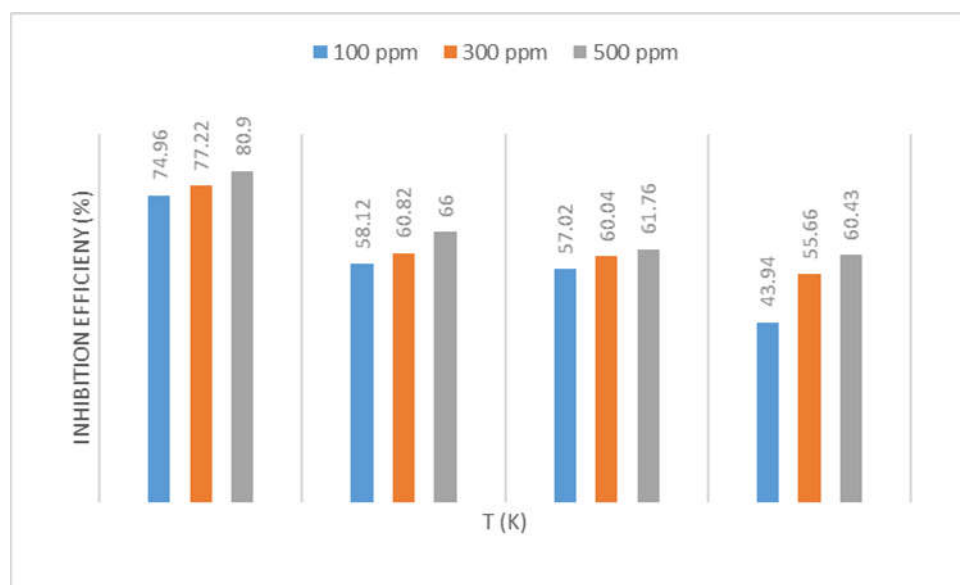
3.2. Corrosion Inhibition Studies

To assess the effect of temperature change on the inhibitive effect of LLE-AgNPs, weight loss measurements were undertaken for 3 hours immersion periods at 303K, 313K, 323K, and 333 K, for blank, 100 ppm, 300 ppm, and 500 ppm concentration of the composite. Both **Figure 8** and **Figure 9** display the results obtained. The inhibition efficiency increased with increase of the inhibitor concentration, but decreased with increase in temperature (**Table 1**). The variation in inhibition efficiency with increasing temperature is a pointer to the physisorptive nature of the composite to the surface of the metal [25].

Table 1. Inhibition Efficiency (%IE) and Degree of Surface Coverage (Ө) on mild steel in 1.0 M HCl in the presence of LLE-AgNPs at various temperatures (K)

| System (ppm)	Inhibition Efficiency at different temperatures (K)			
	303	313	323	333
100	74.96	58.12	57.02	43.94
300	77.22	60.82	60.04	55.66
500	80.90	66.00	61.76	60.43
System (ppm)	Degree of Surface Coverage (Ө)			
100	0.75	0.58	0.57	0.44
300	0.77	0.61	0.60	0.56
500	0.81	0.66	0.62	0.60

Figure 8. Effect of temperature (K) on corrosion inhibition efficiency (%IE) of mild steel in 1.0 M HCl in the presence of LLE-AgNPs

3.3. Polarization measurements

Figure 9 illutstrates the polarization curve of the system, while inhibition efficiencies were calculated from equation 3. The corrosion current density significantly reduced at the introduction of LLE-AgNPs to the test solution, resulting in the displacement of corrosion potential in both anodic and cathodic direction. This result suggests that LLE-AgNPs were adsorbed on the coupon surface to form an inhibitor layer which resulted in the reduction of the corrosion rate, meaning that any inhibition effect will be inhibitor concentration dependent. LLE-AgNPs can therefore be considered as a mixed type inhibitor, but more pronounced impact on the cathodic reaction [26].

Extrapolation of the Tafel slopes gave the electrochemical parameters shown in **Table 2**. The corrosion rate was observed to have significantly reduced at inverse proportion to the concentration of the inhibitor. This is because more of the molecule was adsorbed on the metal surface and the corrosion prevention barrier became denser, preventing the mild steel exposure to the aggressive environment, thereby inhibiting the corrosion rate [27-28]. Corrosion inhibition efficiencies reached as high as 96.44 % with the 500 ppm LLE-AgNPs concentration, when compared with the blank coupon, a trend were consistent with the results obtained from the gravimetric analysis.
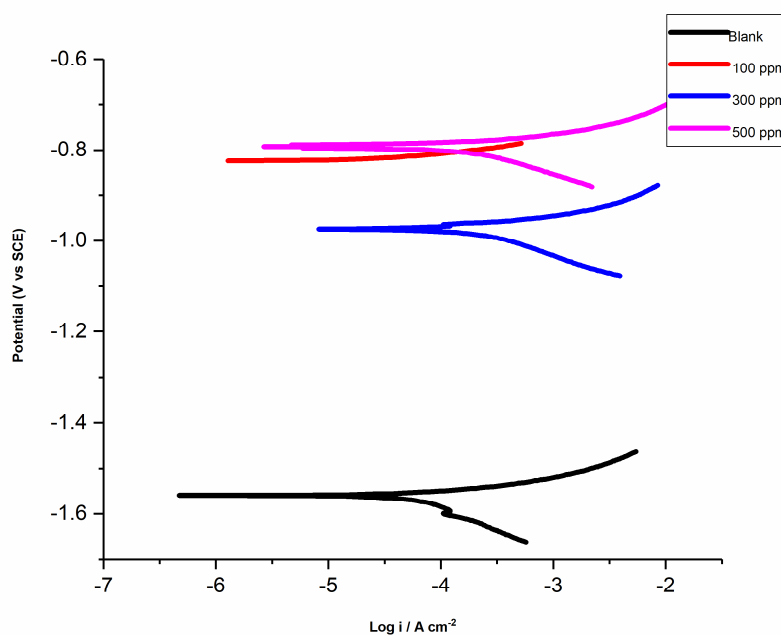
Figure 9. Tafel plot for mild steel in 1.0 M HCl in the absence and presence of LLE-AgNPs

**Table 2.** Tafel parameters for mild steel in 1.0 M HCl in the absence and presence of LLE-AgNPs.

System (ppm)	Ecorr (mV)	jcorr ($\mu A/cm^2$)	βa (V/dec)	βc (V/dec)	CR (mm/year)	%IE
Blank	-1577.20	1404.80	-163.33	63.46	16.32	-
100	-935.66	607.25	-100.47	59.66	7.056	55.77
300	-844.96	83.96	- 47.97	34.63	1.078	93.40
500	-795.27	49.90	- 19.69	25.45	0.580	96.44

3.4. Kinetic and Thermodynamic Studies

As depicted in **Figure 10**, the corrosion rate of mild steel coupons in 1.0 M HCl decreased with increasing concentration of LLE-AgNPs, but increased with rise in temperature. This decrease in corrosion rate with rise in concentration suggests an increase in the fraction of the mild steel covered by the adsorbed constituent of the composite, providing a barrier that prevented further corrosion, a deduction that is corroborated by the increase in the values of the degree of surface coverage shown in **Table 1** [29]. This trend is a consequence of the physical adsorption (physisorption) of the LLE-AgNPs molecules onto the corroding metal surface. As the temperature is raised, there is a decline in the amount of the inhibitor molecules adsorbed causing their partial desorption and increased corrosion rate [30].
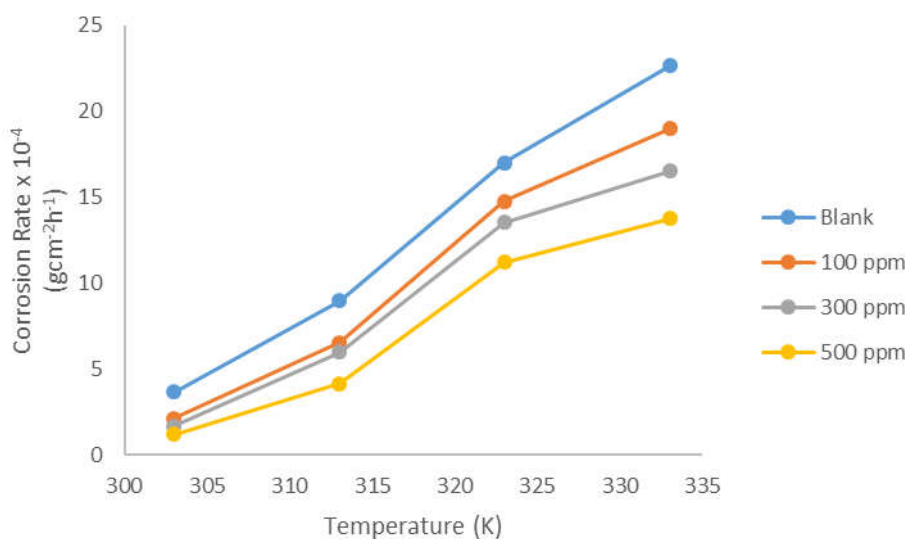
Figure 10. Dependence of corrosion rate of mild steel in 1.0 M HCl on temperature (K) in the absence and presence of LLE-AgNPs

Metal corrosion in aggressive solution requires a minimum energy input for which the corrosion reaction cannot proceed until the energy barrier is surmounted [31-32]. Arrhenius equation (equation 4) describes the variation of corrosion rate with temperature, where CR is the corrosion rate, T is the absolute temperature, A is Arrhenius pre-exponential frequency factor, R is the universal gas constant, and Ea is a quantity characteristic of the adsorption process with dimensions of that of energy known as activation energy, which is used to describe the kinetics of LLE-AgNPs adsorption from the Arrhenius plot of log CR against 1/T (**Figure 10)**.

$$\log CR = \log A - \frac{Ea}{2.303RT} \qquad (4)$$
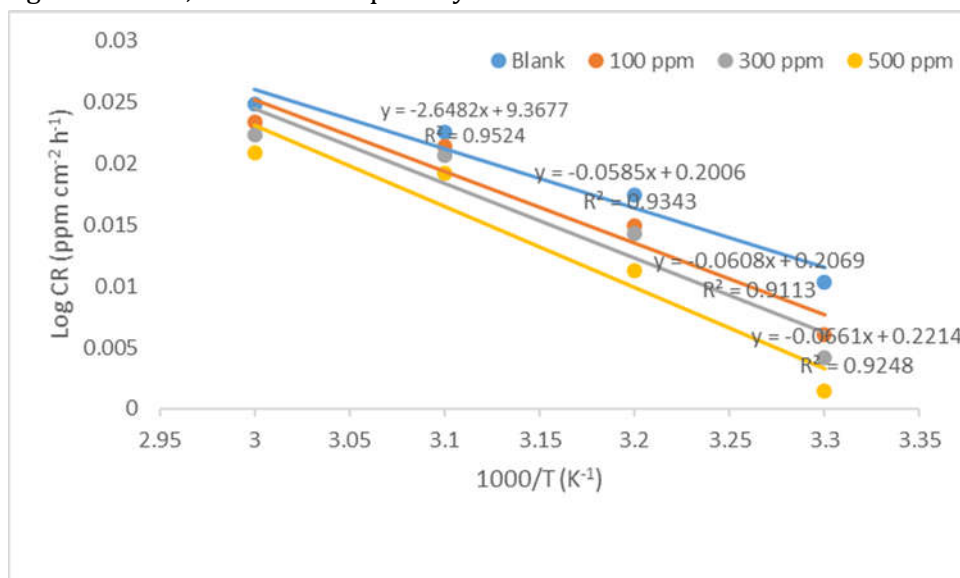
Figure 11. Arrhenius plot of log CR against 1/T for the corrosion inhibition of mild steel in hydrochloric acid

The thermodynamic activation parameters obtained from the plots are listed in **Table 3**. The lowest value of Ea (22.017 KJmol^{-1}) was obtained in the absence of LLE-AgNPs, which increased consistently with increase in the concentration of LLE-AgNPs, with the highest values of 30.004 KJmol^{-1} in the presence of 500 ppm of the inhibitor. The adsorbed LLE-AgNPs has provided an energy barrier and mass transfer to the change, leading to reduction in corrosion rate

[33]. The value of Ea greater than 80 KJmol^{-1} has been reported to indicate chemical adsorption, as opposed to physical adsorption with Ea less than 80 KJmol^{-1} [34-35]. From the experimentally determined Ea values which are all less than 80 KJmol^{-1}, it is evidenced that the additives were physically adsorbed on the coupons. The multilayer protective coverage on the entire surface of the mild steel can therefore be considered to be obtained.
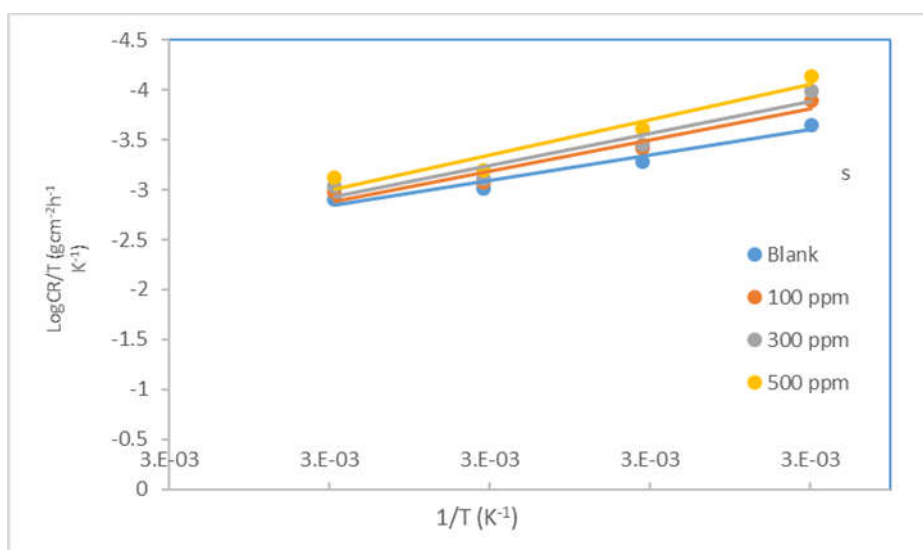
Figure 12. Transition state plots for mild steel corrosion in the absence and presence of LLE-AgNPs

The enthalpy and entropy of adsorption of the inhibitor is related to the corrosion rate of a metal by equation 5.

$$CR = \frac{RT}{Nh} \exp\left(\frac{\Delta S_{ads}}{R}\right) \exp\left(\frac{-\Delta H_{ads}}{RT}\right) \qquad (5)$$

With CR representing the corrosion rate of the mild steel, while R and N stands for gas constant Avogadro's number, respectively, Planck's constant and temperature are denoted with h and T, respectively. The entropy adsorption of the inhibitor on a metal is ΔS_{ads} and ΔH_{ads} is the enthalpy of adsorption of the inhibitor on a metal [36].

Equation (5) can be transformed into a linear form by taking logarithm of both sides of the equation to obtain equation (6),

$$\log\left(\frac{CR}{T}\right) = \log\left(\frac{R}{Nh}\right) + \left(\frac{\Delta S_{ads}}{2.303R}\right) - \left(\frac{\Delta H_{ads}}{2.303RT}\right) \qquad (6)$$

From equation (6), a straight line graph of log (CR/T) versus 1/T was obtained (**Figure 12),** giving $\Delta H_{ads}/2.303R$ and (log(R/Nh) + $\Delta S_{ads}/2.303R$), as the slope and intercept, respectively. The activation parameters evaluated are reported in **Table 3.** The endothermic nature of the mild steel dissolution in 1.0 M HCl is confirmed by the positive values of the enthalpy of activation for the inhibitor established. Likewise, the entropies of adsorption were positive for the composite, showing the associative mechanism of the activation complex, a reaction which was also proven to be spontaneous and feasible. These results were in excellent agreement with the reports of previous works [37].

Table 3. Thermodynamic parameters

System (ppm)	Ea (kJ mol^{-1})	ΔH (J mol^{-1})	ΔS (kJ mol^{-1})
Blank	22.017	6.227	0.317
100	26.538	8.157	0.328
300	27.601	8.470	0.331
500	30.004	8.881	0.334

3.5. Adsorption Isotherm

Of the various isotherms tested, Langmuir adsorption isotherms was found to be best fit in which case the linear regression coefficients (R^2) was close to unity. According to the assumption of Langmuir adsorption isotherm, fixed number of adsorption sites is contained by the solid surfaces and each site holds one adsorbed species [38].

$$\log\left(C/_\theta = \log C - \log K\right) \qquad (7)$$

Langmuir isotherm can be written as indicated in **equation 7**, in which K is the adsorption equilibrium constant and θ is the degree of surface coverage of the inhibitor. A straight line graphs were obtained when the log (C/θ) were plotted against the values of log C [39].

Langmuir isotherm gives a straight line between C/θ *vs* C, [40]. The values of ΔG and Kads obtained from **Figure 13** are listed in **Table 4**. From the negative values obtained for ΔG, the adsorption process proceeded spontaneously and is physically adsorbed to the mild steel surface.

Generally, the value of ΔG°$_{ads}$ less or equal to −20 kJ mol^{-1} signifies physisorption, while chemisorption is signified by values more negative than −40 kJ mol^{-1} [41-42].
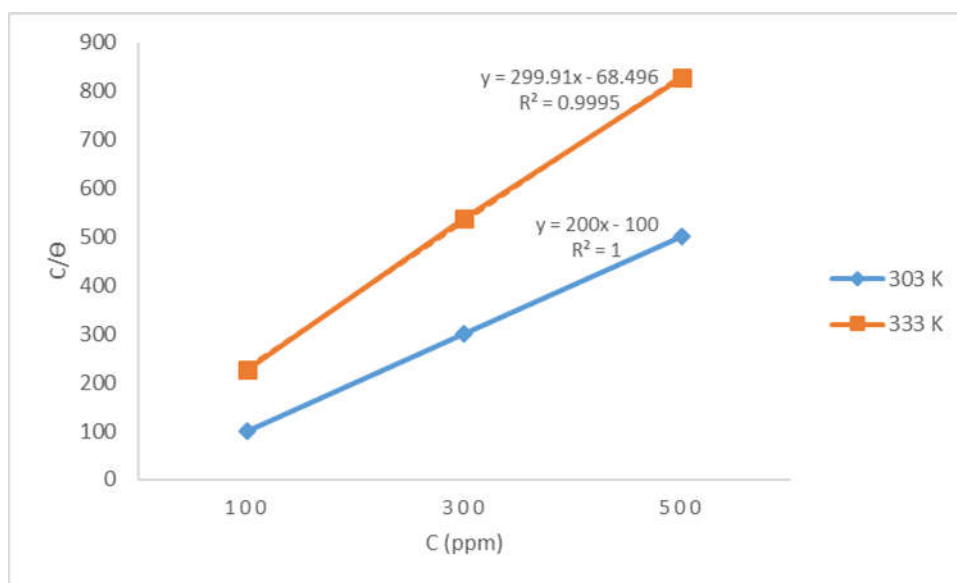
Figure 13. Langmuir isotherm for the adsorption of LL onto mild steel surface in 1.0 M HCl at 303K and 333K respectively

Table 4. Langmuir isotherm parameters obtained

Temperature (K)	R^2	Slope	Intercept	K$_{ads}$	ΔG$_{ads}$ (kJ/mol)
303	1.000	200.000	100.000	0.010	-4.318
333	0.999	299.910	68.496	0.015	-0.583

4. Conclusion

The use of *Lonchocarpus laxiflorus* extract as a reducing agent for silver nitrate to nanoparticles, and its effectiveness as a cheap, economical, and eco-friendly inhibitor of corrosion of mild steel in 1.0 M HCl has been reported. The linear polarization studies revealed that the LLE-AgNPs affected both the cathodic and anodic processes, hence, is a mixed type inhibitor. The obtained values of activation energies (Ea) indicated that the LLE-AgNPs adsorbed on the mild steel surface through the mechanism of physisorption. The positive values of enthalpy and entropy of activation signified that the LLE-AgNPs adsorbed endothermically on the metal surface and that the activation complex in the rate determining step represents the associative mechanism. Comparatively, LLE-AgNPs is a more effective inhibitor of corrosion in 1.0 M HCl than only LL extract.

Acknowledgement

Conflict of Interests

No conflict of interests.

References

[1]   G.A. Ijuo, A.M. Orokpo, P.N. Tor, Effect of *Spondias mombin* Extract on the Corrosion of Mild Steel in Acid Media, *Chemrj*, 3 (2018) 64-77

[2]   N.AI Otaibi, H.H. Hammud, Corrosion Inhibition Using Harmal Leaf Extract as an Eco-Friendly Corrosion Inhibitor, *Molecules*, 26 (2021) 7024. https://doi.org/10.3390/molecules26227024

[3] A. Ahmed, Corrosion inhibition effect of 2-N-phenylamino-5-(3-phenyl-3-oxo-1-propyl)-1,3,4-oxadiazole on mild steel in 1 M hydrochloric acid medium:Insight from gravimetric and DFT investigations, *Materials Science for Energy Technologies*, 4 (2021) 398-406

[4] A.E. Edidiong, K. Doga, B.E. Ituen, S.A. Umoren. Synthesis, Characterization and anticorrosion property of olive leaves extract titanium nanoparticles composite, *J of Adhesion Sci and Tech*, (2018). DOI: 10.1080/01694243.2018.1445800

[5] D.C. Benjamin, A.L. Richard, H.R. David, Corrosion control and monitoring; a program management guide for selecting materials. Advanced Materials, Manufacturing and Testing Information Analysis Center (AMMTIAC), New York, USA, (2006) 1-19.

[6] M. Chukwuma, https://allafrica.com/stories/201711160049.html, 2017.

[7] O.O. Akinyem, C.N. Nwaokocha, A.O. Adesanya, Evaluation of Corrosion Cost of Crude Oil Processing Industry, *Journal of Engineering Science and Technology*, 7 (2012) 517-528

[8] G.A. Ijuo, H.F. Chahul, I.S. Enej, Kinetic and thermodynamic studies of corrosion inhibition of mild steel using *Bridelia ferruginea* extract in acidic environment, *J. Adv. Electrochem*, 2 (2016) 107–112.

[9] D. Nayak, S. Ashe, P.R. Rauta, Bark extract mediated green synthesis of silver nanoparticles: Evaluation of antimicrobial activity and antiproliferative response against osteosarcoma, *Mater Sci Eng C*, 58 (2016) 44–52.

[10]   M.A. Ayman, A.A. Hamad, G.A. El-Mahdy, O.E. Abdel-Rahman, Application of Stabilized Silver Nanoparticles as Thin Films as Corrosion Inhibitors for Carbon Steel Alloy in 1M Hydrochloric Acid, *Hindawi Publishing Corporation J nanomaterials*, (2013). https://doi.org/10.1155/2013/580607

[11]   T.W. Quadri, L.O. Olasunkanmi, O.E. Fayemi, Zinc oxide nanocomposites of selected polymers: synthesis, characterization, and corrosion inhibition studies on mild steel in HCl solution, *ACS Omega*, 2 (2017) 8421–8437.

[12]   M.M. Solomon, H. Gerengi, S.A. Umoren, Gum Arabic – silver nanoparticles composite as a green anticorrosive formulation for steel corrosion in a strong acid media, *Carbohyd Polym*, 181 (2018) 43–55.

[13] T.B. Asafa, M.O. Durowoju, K.P. Madingwaneng, S. Diouf, E.R. Sadiku, M.B. Shongwe, P.A. Olubambi, O.S. Ismail, M.T. Ajala, K.O. Oladosu, Gr–Al composite

reinforced with Si₃N₄ and SiC particles for enhanced microhardness and reduced thermal expansion. *Appl. Sci.* (2020) 1026. https://doi.org/10.1007/s42452-020-2838-5

[14] D. N. Hans, African Ethnobotany: Poison and Drugs Chemistry, Pharmacology and Toxicology, CRC Press, *London*, 25 (1996) 1-5.

[15] G.A. Ijuo, H.F. Chahul, and I.S. Eneji, Corrosion inhibition and adsorption behavior of Lonchocarpus laxiflorus extract on mild steel in hydrochloric acid, *Ew J Chem Kinet*, 1 (2016) 21-30.

[16] K. Shameli, M. Bin Ahmad, E.A.J. Al-Mulla EA, N.A. Ibrahim, P. Shabanzadeh, A. Rustaiyan, Y. Abdollahi, S. Bagheri, S. Abdolmohammadi, M.S. Usman, M. Zidan. Green biosynthesis of silver nanoparticles using Callicarpa maingayi stem bark extraction, *Molecules*, 17 (2016) 8506-17. doi: 10.3390/molecules17078506.

[17] E.F.Olasehinde, S.J. Olusegun, A. S Adesina, S.A Omogbehin, H. Momoh-Yahayah, Inhibitory action of Nicotiana tobacum extracts on the corrosion of mild steel in HCl: adsorption and thermodynamic study, *Natural Science*, 11 (2013) 83-90

[18] M. Salari, M.S. Khiabani, R.R. Mokarram., B. Ghanbarzadeh, H.S. Kafil, Development and evaluation of chitosan based active nanocomposite films containing bacterial cellulose nanocrystals and silver nanoparticles, *Food Hydrocolloids*, 84 (2018) 414-423

[19] G. Maduraiveeran, R. Ramaraj, Silver nanoparticles embedded in functionalized silicate sol-gel network film as optical sensor for the detection of biomolecules, *J Anal Chem*, 68 (2015) 241-8.

[20] A.M. Whelan, M.E. Brennan, W.J. Blau, J.M. Kellya, Enhanced third-order optical nonlinearity of silver nanoparticles with a tunable surface plasmon resonance, *J Nanosci Nanotechnol*, 4 (2015) 66-8

[21] R. Desai, V. Mankad, S.K. Gupta, P.K. Jha, Size distribution of silver nanoparticles: UV-visible spectroscopic assessment. *Nanosci Nanotechnol Lett*, 4(2015) 30-4.

[22] R. He, X. Qian, J. Yin, Z. Zhu, Preparation of polychrome silver nanoparticles in different solvents, *J Mater Chem*, 12 (2015) 3783-6.

[23] A.M. Law, W.D. Kelton, Simulation Modelling and Analysis. 2nd Edition, McGraw-Hill, New York, 1991

[24] O. Benhabiles, F. Galiano, T. Marino, H. Mahmoudi, H. Lounici, A. Figoli, Preparation and Characterization of TiO2-PVDF/PMMA Blend Membranes Using an Alternative Non-Toxic Solvent for UF/MF and Photocatalytic Application, *Molecules*, 24 (2019) 724. doi:10.3390/molecules24040724

[25] J. Bagyalakshmi, H. Haritha, Green Synthesis and Characterization of Silver Nanoparticles Using *Pterocarpus marsupium* and Assessment of its *In vitro* Antidiabetic Activity, *AJADD*, 5 (2017), 118-130.

[26] M.M Ihebrodike, C.N. Michael, B.O. Kelechukwu, L.A Nnanna, M.A. Chidiebere, F.C. Eze, E.E.Oguzie, Experimental and theoretical assessment of the inhibiting action of *Aspilia africana* extract on corrosion aluminium alloy AA3003 in hydrochloric acid, J Mater Sci, 47 (2019) 2559-2572. DOI: 10.1007/s10853-011-6079-2

[27] V. Grudić, I. Bošković, A. Gezović, Inhibition of Copper Corrosion in NaCl Solution by Propolis Extract, *Chem. Biochem. Eng. Q.*, 32 (2018) 299–305.

[28] M.E. Sadeghi, F.T. Shahrabi, J. Neshati, 2-Butyne-1,4-diol as a novel corrosion inhibitor for API X65 steel pipeline in carbonate/bicarbonate solution, *Corros Sci*, 54 (2012) 36–44.

[29] C. Shen, V. Alvarez, J.D.B. Koenig, and J. Luo,. Gum Arabic as corrosion inhibitor in the oil industry: experimental and theoretical studies, Corrosion Engineering, *Science and Technology*, 54 (2019) 444-454

DOI: 10.1080/1478422X.2019.1613780

[30] M.M. Ihebrodike, A. U. Anthony A.U., B.O. Kelechukwu, G.A. Alozie, The inhibition Effect of *Solanummelongena L*, leaf extract on the corrosion of aluminium in tetraoxosulphate (vi) acid, *Afr. J. Pure Appl. Chem*, 4 (2010) 158-165.

[31] B.A. Sami, On the corrosion inhibition of carbon steel in 1 M HCl with a pyridinium-ionic liquid: chemical, thermodynamic, kinetic and electrochemical studies, *RSC Adv*, 7 (2017) 36688

[32] N.O. Eddy, A.E. Patricia, P.A.P. Mamza, Ethanol extract of Terminalia catappa as a green inhibitor for the corrosion of mild steel in H₂SO₄. *Green Chem Lett Rev*, 2 (2009) 223-231.

[33] N.O. Eddy, E.E. Ebenso, Corrosion inhibition and adsorption properties of ethanol extract of Gongronema latifoliumon mild steel in H₂SO₄, *Pigment and Resin Technology*, 39 (2010) 77-83.

[34] A.O. Okewale, O.A. Adesina, Kinetics and Thermodynamic Study of Corossion Inhibition of Mild Steel in 1.5 M HCl Medium using Cocoa Leaf Extract as Inhibitor, *J. Appl Sci. Environ, Manage*, 24 (2010) 37-47

[35] M. Ismail, A.S. Abdulrahman and M.S. Hussain, Solid waste as environmental benign corrosion inhibitors in acid medium, *Int. J. Engg. Sci. Technol*, 3 (2011) 1742-1748.

[36] N.B. Iroha, N.J. Maduelosi, Corrosion Inhibitive Action and Adsorption Behaviour of Justicia Secunda Leaves Extract as an Eco-Friendly Inhibitor for Aluminium in Acidic Media, *Biointerface Research in Applied Chemistry*, 11 (2021) 13019–13030. https://doi.org/10.33263/BRIAC115.1301913030

[37] E.C. Ogoke, S.A. Odoemelam, B.I. Ita, N.O. Eddy, Adsorption and inhibitive properties of clarithromycin for the corrosion of zinc in 0.01 to 0.05 M H_2SO_4 Port, *Electrochim. Acta*, 27 (2009) 713-724*.

[38] E.F. Olasehinde, S.J. Olusegun, A.S. Adesina, S.A. Omogbehin, H. Momoh- Yahayah Inhibitory action of *Nicotiana tobacum* extracts on the corrosion of mild steel in HCl: adsorption and thermodynamic study, *Nat. Sci.*, 11 (2013) 83-90.

[39] O. Oyeneyin, D. Akerele, N. Ojo, O. Oderinlo, Corrosion Inhibitive Potentials of some 2H-1-benzopyran-2-one Derivatives- DFT Calculations, *Biointerface Research in Applied Chem*, 6 (2021) 13968–13981. https://doi.org/10.33263/BRIAC116.1396813981

[40] N.O. Eddy, E.E. Ebenso, Corrosion inhibition and adsorption properties of ethanol extract of *Gongronema latifolium*on mild steel in H_2SO_4, *Pigm. Resin Tech*, 39 (2010) 77-83.

[41] E.E. Oguzie, Y. Li, F.H. Wang, Corrosion inhibition and adsorption behaviour of methionine on mild steel in sulfuric acid and synergistic effect of iodide ion, *J. Colloid Interf. Sci.*, 310(2007) 90-98.

[42] N.O. Eddy, A.S. Ekop, Inhibition of corrosion of zinc in 0.1 M H2SO4 by 5- amino-1- cyclopropyl-7-[(3r,5s) 3,5dimethylpiperazin-1-yl]-6,8-difluoro-4-oxo quinolone-3carboxylic acid, *Mat. Sci. Ind. Jour.*, 4s (2007) 2008-2016.

[43] R. Saratha, D. Saranya, H.N. Meenakshi, R. Shyamala, Enhanced corrosion resistance of Tecoma stans extract on the mild steel in 0.5 M H_2SO_4 solution, *Int. J. Current Res*, 2 (2011) 092-096.